Brain Space

van Es, D.M.

2019

document version
Publisher's PDF, also known as Version of record

Appendix C

Supplementary Figures for Chapter 4

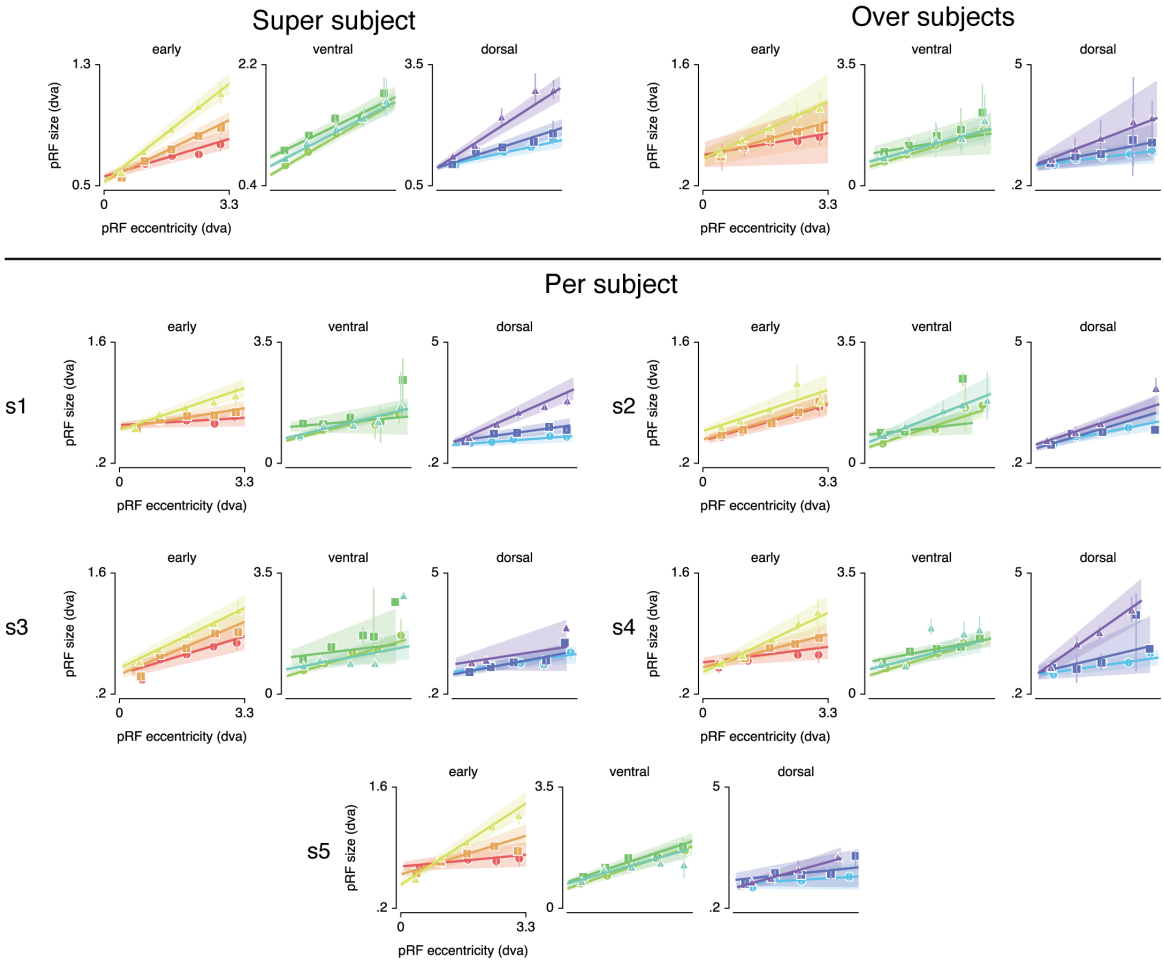

Figure 2 - figure supplement 1. Eccentricity-size relations for all statistical methods. This shows that eccentricity size relations are positive in all ROIs for both the 'super subject' method (Table 1) and the 'over subjects' method (Table 11). Regarding the individual subjects, we find that although slopes between eccentricity and size were positive in all ROIs in all subjects, this was not always significant with α of .05. Yet, this occurred for maximally one out of five subjects in some ROIs: in MT+ in s3 ($p = .058$), in V3AB ($p = .073$) and IPS0 ($p = .078$) in s5 and VO in s1 ($p = .146$)). In the 'super subject' and 'per subject' methods error bars denote 95% CI over voxels; in the 'over subjects' method, error bars denote 95% CI over subjects. See Methods section for definition of 'super subject', 'over subjects' and 'per subject' methods.

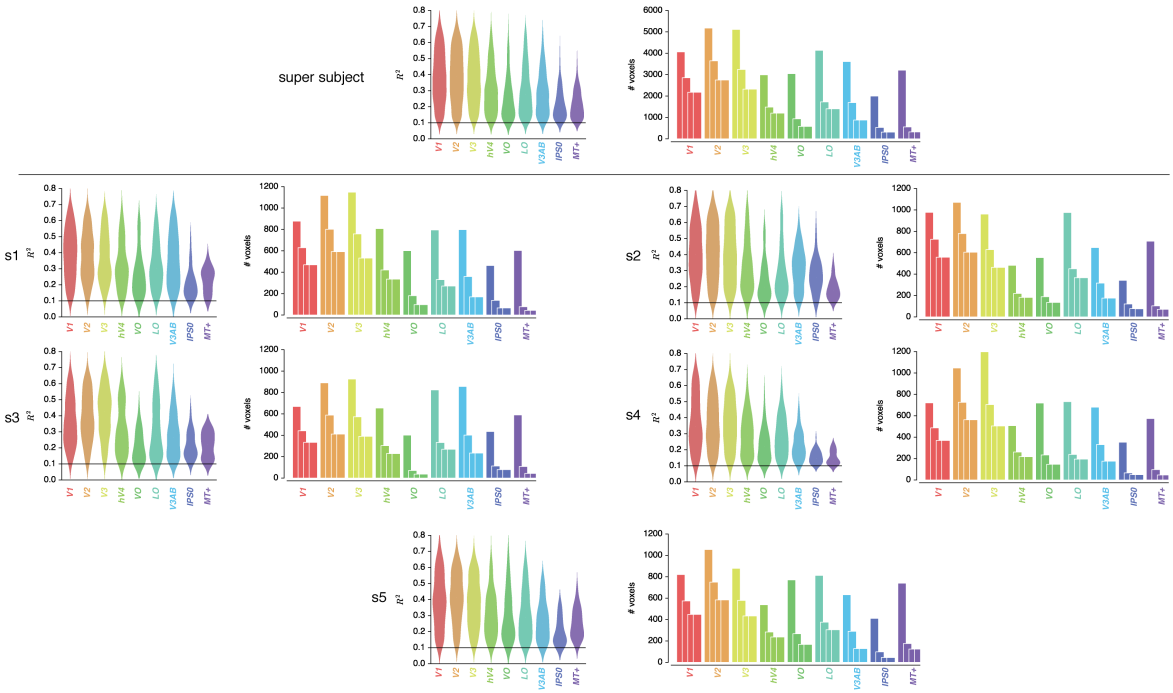

Figure 2 - figure supplement 2. The violin plots depict the distribution of explained variance across voxels for the different ROIs and for all subjects. The horizontal line at .10 indicates the exclusion criterion (voxels with explained variance lower than .10 are also excluded from these violin plots). The bar plots show the number of voxels that survived different rejection criteria for all ROIs and for all subjects. The first bar of each ROI depicts all voxels within the retinotopically defined mask where explained variance is larger than > .01. This serves as a baseline of 'all' voxels within that area. The second bar depicts all voxels where explained variance is larger than > .10 (the criteria used in all subsequent analyses). The third bar depicts the number of voxels where explained variance is > .10 and where pRF eccentricity was smaller than 3.3 dva. The last bar depicts the number of voxels where explained variance is > .10, where pRF eccentricity is < 3.3 dva and where pRF size is < 7.2 dva. The figure shows that most voxels are rejected either because their explained variance was too low or because they fell outside of the stimulus region. The additional pRF size rejection criterion virtually did not reject any additional voxels. The last bar of the 'super subject' is what is shown in the main figure. See Methods section for definition of 'super subject' and 'per subject' methods.

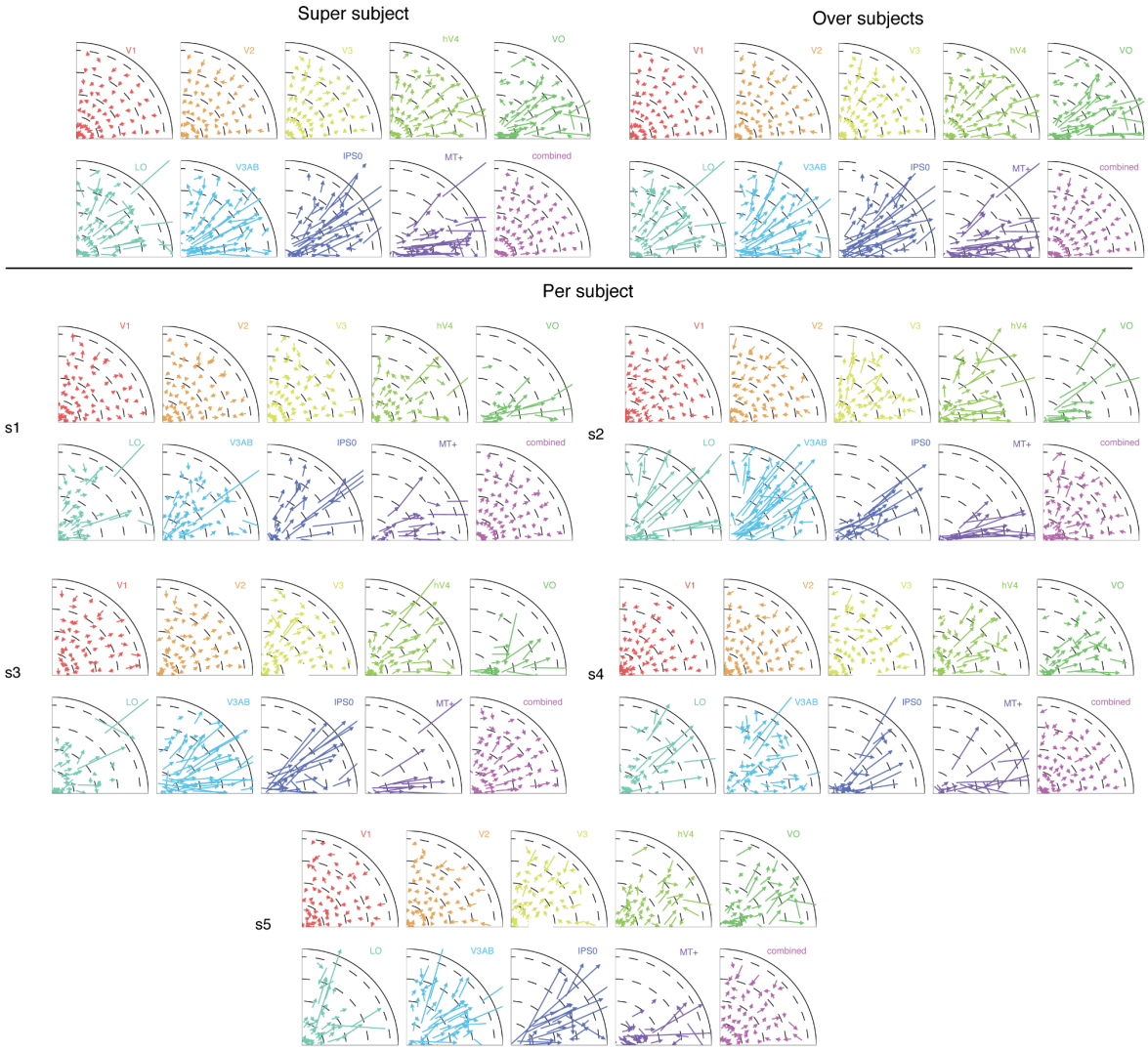

Figure 3 - figure supplement 1. pRF shift plots for the different statistical methods. Shift vectors run from the Attend Fixation to the Attend Stimulus pRF location. This figure indicates that the shift patterns seen in the 'super subject' are almost identical to the 'over subjects' method, and highly agree with the individual subject figures. Note the radial shift direction that is readily apparent in all ROIs in all subjects. Also note how the combined ROI clearly shows parafoveal pRFs shifting toward the periphery and peripheral pRFs shifting toward the fovea across subjects. Finally, the absence of pRFs near the vertical meridian in data from all subjects in VO, IPS0 and MT+ highlight the overrepresentation of the horizontal meridian that is found in all ROIs (see Tables 3, 14 and 15). See Methods section for definition of 'super subject', 'over subjects' and 'per subject' methods.

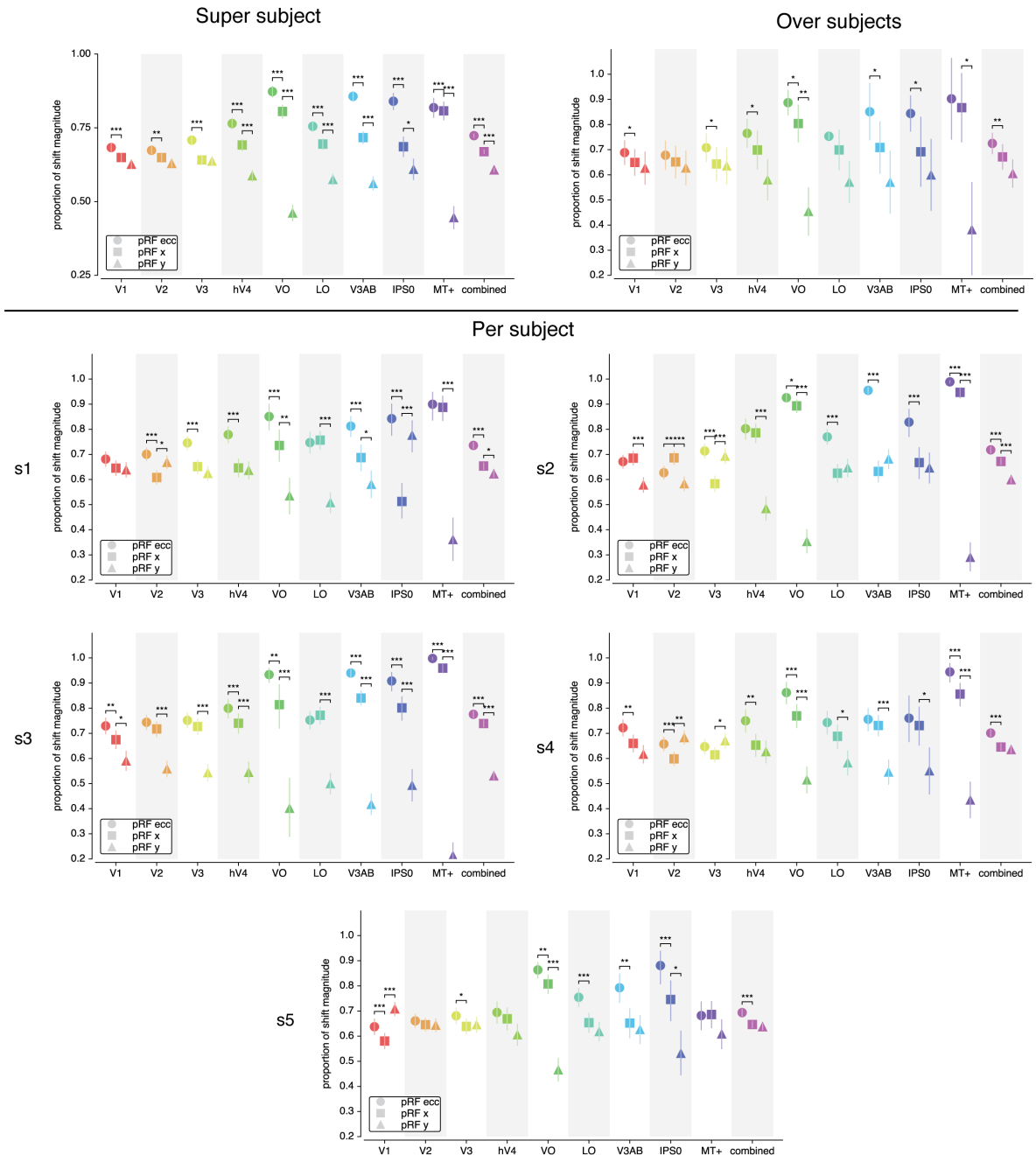

Figure 3 - figure supplement 2. pRF shift directions for the different statistical methods. The 'over subjects' panel replicates the 'super subject' results, namely that shifts are best explained by eccentricity changes, followed by changes in pRF x and finally in pRF y in all ROIs (see Table 2). The dominance of eccentricity over x changes was significant in all individual subjects ('per subject' method) in the combined ROI, and in at least 2 (but often 5) subjects in all other ROIs (see Table 13). The individual subject evidence also replicates the finding that pRFs shifted more in the x compared to y directions in hV4/VO/LO/V3AB/IPS0/MT+ and in the combined ROI (i.e. significant in at least 2/5 of subjects; see Table 12). The dominance of x over y shifts

was explained from a non-uniformity in the distribution of pRF polar angle (i.e. overrepresentation of horizontal meridian, see Table 3). This was also found in most individual subjects for most ROIs (see Tables 14 and 15). Single, double and triple asterisks indicate significant differences at $p < .05$, .01 and .001 respectively. In the 'super subject' and 'per subject' methods error bars denote 95% CI of data over voxels; in the 'over subjects' method, error bars denote 95% CI over subjects. See Methods section for definition of 'super subject', 'over subjects' and 'per subject' methods.

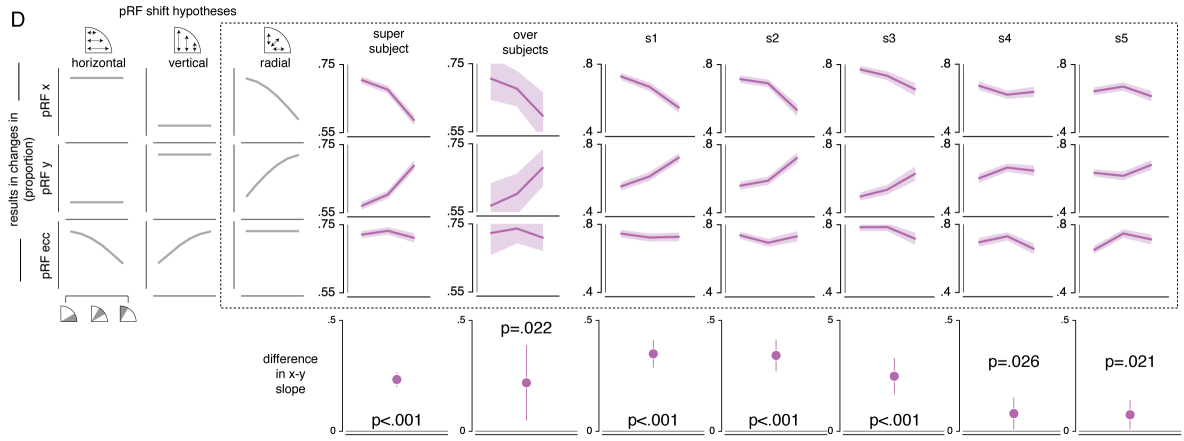

Figure 3 - figure supplement 3. pRF x, y and eccentricity position shifts as a function of polar angle. The data from all statistical methods closely matches the radial shift direction hypothesis, showing strongest pRF x shifts close to the horizontal meridian, strongest pRF y shifts close to the vertical meridian and no polar angle dependence of pRF eccentricity shifts. This is evidenced by a more positive slope of y change over polar angle compared to slope of x change over polar angle in the 'super subject' method (see main text for statistics), for the 'over subjects' method (slope difference = 0.219, $t_{(4)}$ = 3.616, p = 0.022, Cohen's d = 1.808). Error bars reflect 95% CIs across voxels in the 'super subject' and 'per subject' methods, and across subjects in the 'over subjects' method. See Methods section for definition of 'super subject' and 'over subjects' methods.

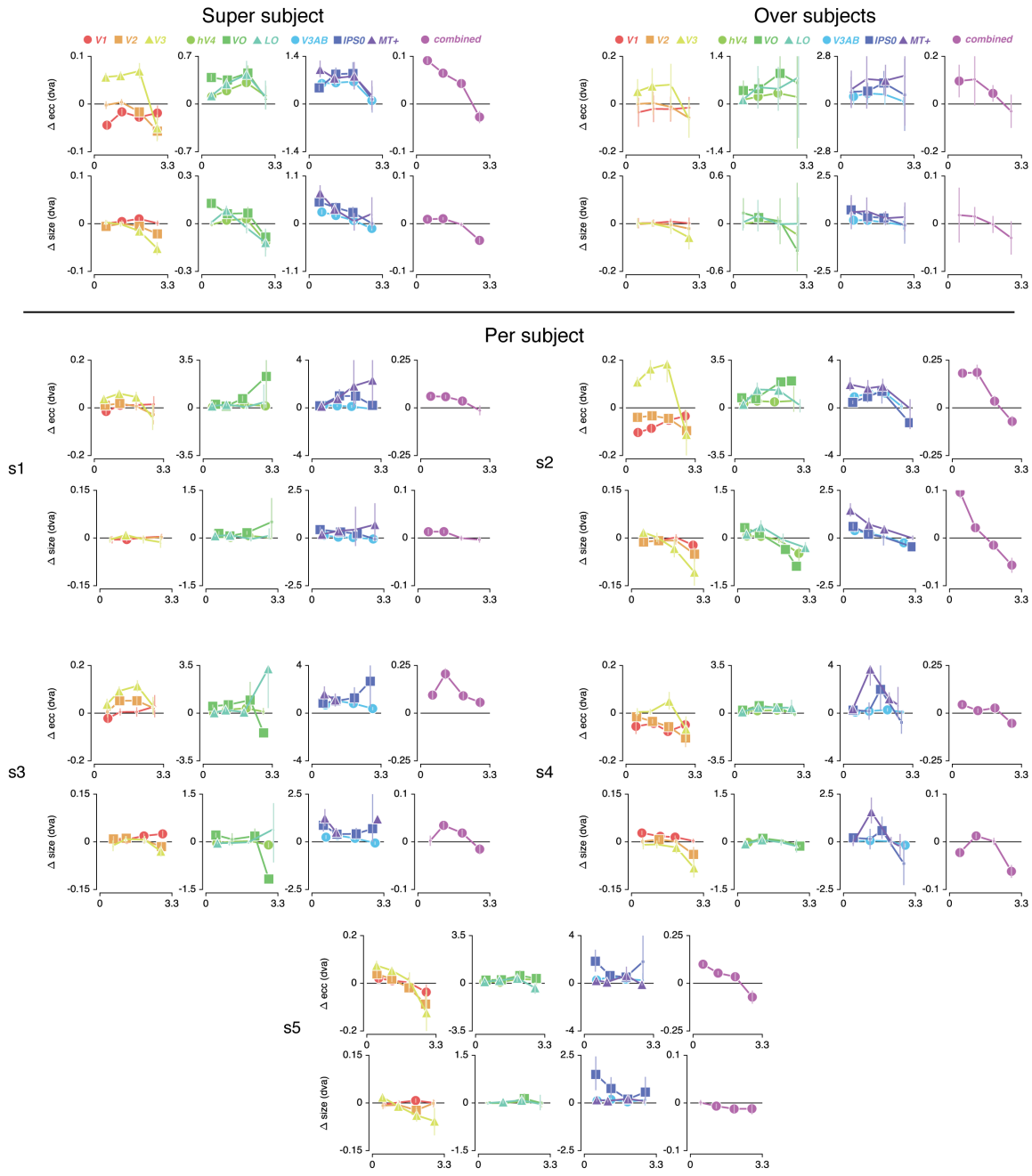

Figure 4 - figure supplement 1. Difference between Attend Stimulus and Attend Fixation pRF eccentricity and size as a function of Attend Fixation eccentricity (see Tables 4-7 and 16-23). The data shows a transition from inwards to outwards shifts across the visual hierarchy in all subjects. Additionally, the progressions of change over eccentricity show some variability within ROIs between subjects. Finally, data from the combined ROI in most subjects reveals that parafoveal pRFs tend to shift away from the fovea and increase in size, while peripheral pRFs tend to shift toward the fovea and decrease in sizes. Error bars reflect 95% CIs across voxels in the 'super subject' and 'per subject' methods, and across subjects in the 'over subjects' method.

Increased marker size indicates significance with $p < .05$ (FDR corrected for 'super subject'). See Methods section for definition of 'super subject', 'over subjects' and 'per subject' methods.

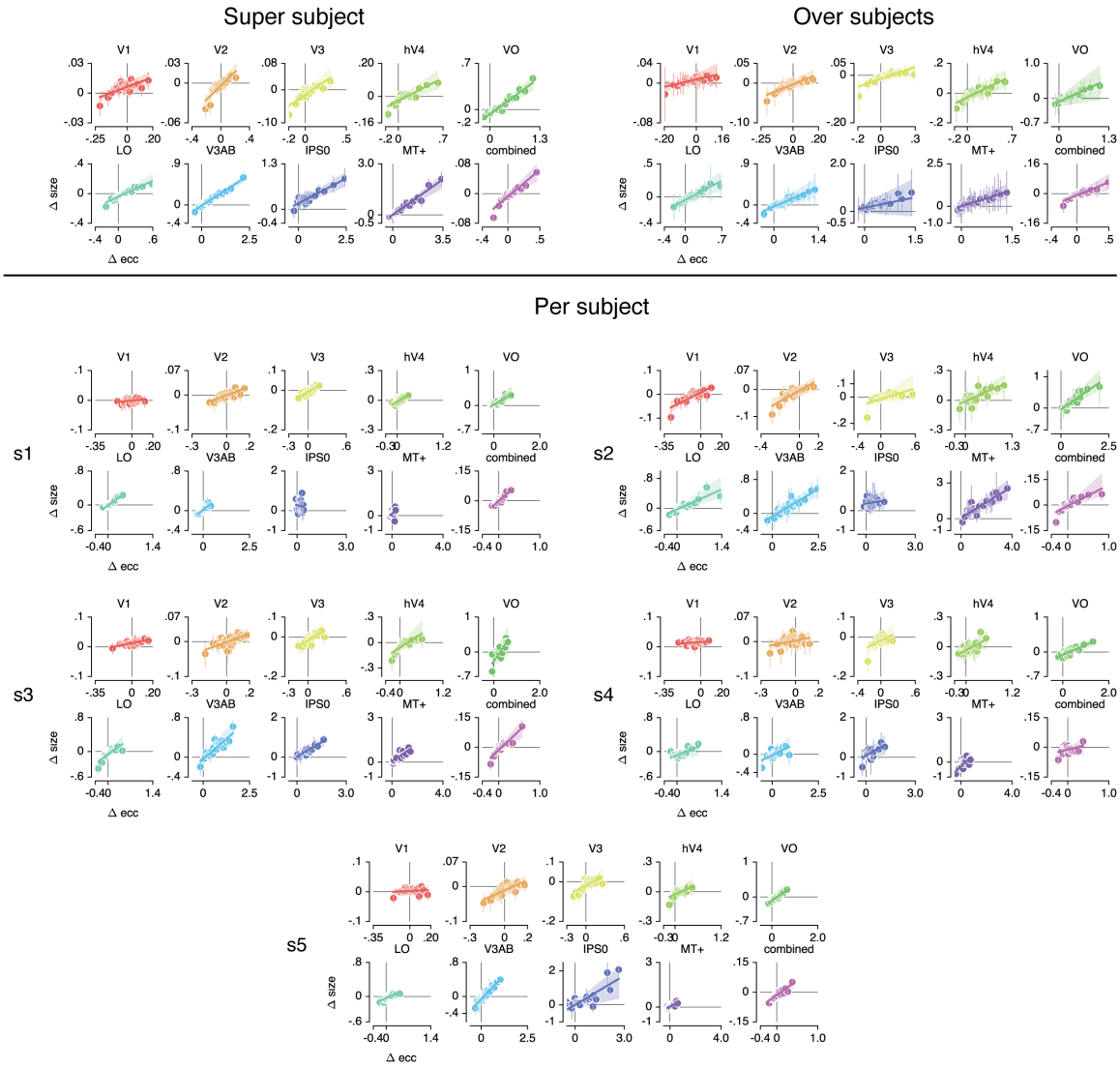

Figure 4 - figure supplement 2. Changes in pRF eccentricity and size were correlated in all ROIs. In the 'over subjects' method, we find that pRF eccentricity and size changes are significant in all ROIs except IPSO (although p = .070). In the 'per subject method', we find such a significant correlation in at least 2 (but often 5) subjects (see Table 24). Error bars reflect 95% CIs across voxels in the 'super subject' and 'per subject' methods, and across subjects in the 'over subjects' method. See Methods section for definition of 'super subject', 'over subjects' and 'per subject' methods.

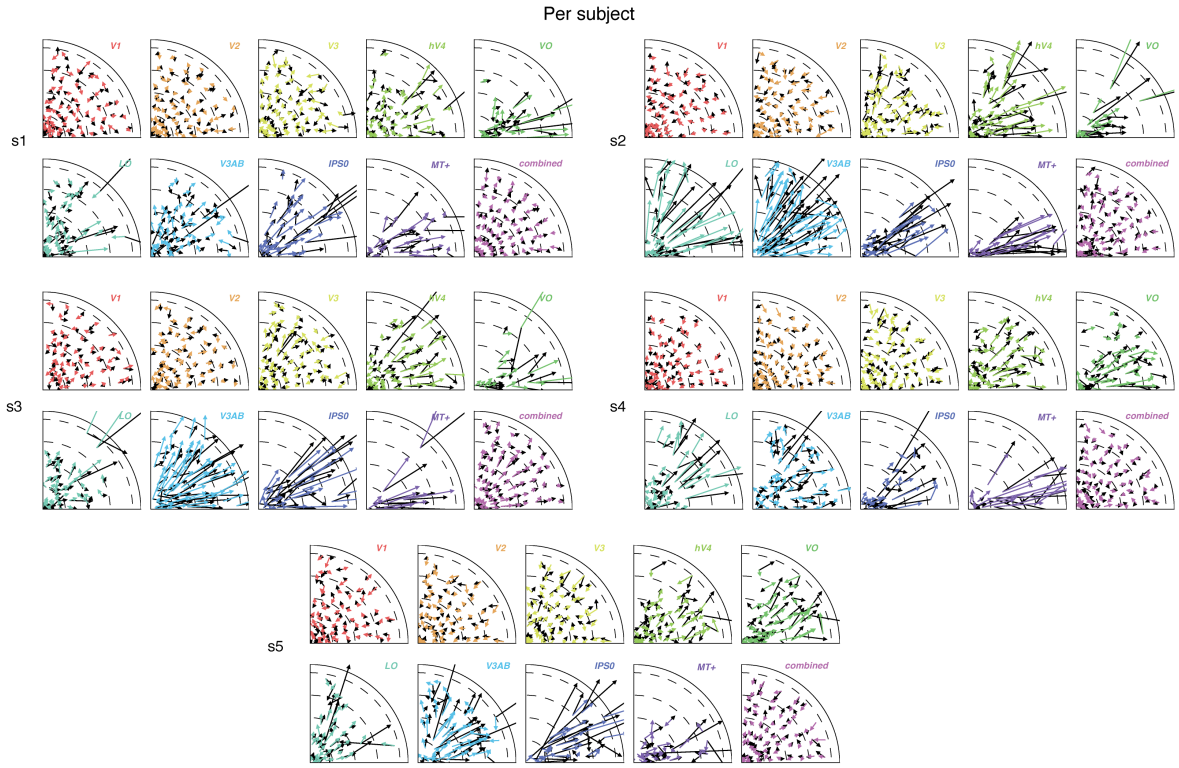

Figure 5 - figure supplement 1. Attentional gain field modeling results for each subject. Arrows depict observed (black) and predicted (color) pRF shifts. This shows that the model closely captured the data in all individual subjects. Each dashed line describes one degree of visual angle of eccentricity.

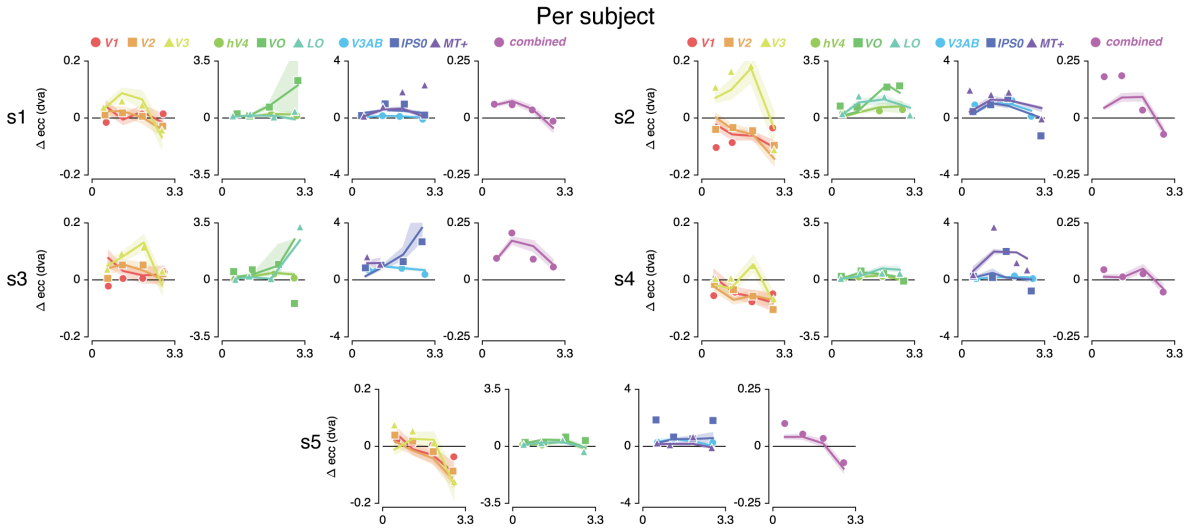

Figure 5 - figure supplement 2. Attentional gain field modeling results for each subject. Observed (markers) and predicted (solid lines) pRF eccentricity difference between Attend Fixation and Attend Stimulus conditions for each subject. This shows that although individual subjects show some variation in the changes in pRF eccentricity across eccentricity, this is well captured by the attentional gain field model. This suggests that individual differences in average pRF changes are not the result of a differential attentional mechanism operating between subjects, but rather that this is due to known individual differences in baseline distribution of pRF parameters (e.g. see Figure 2 – figure supplement 1). Shaded areas indicate 95% CI over voxels.

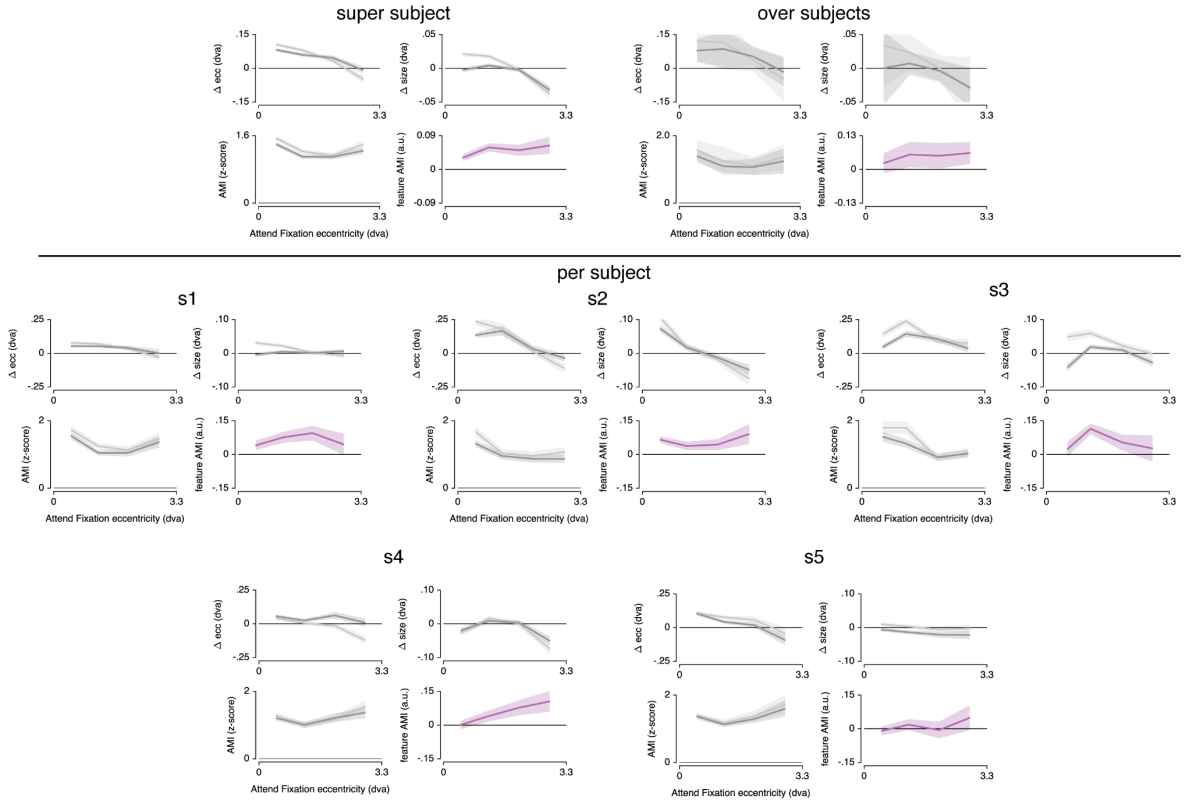

Figure 6 - figure supplement 1. Differences in pRF eccentricity and size relative to the Attention Fixation condition, for both the Attend Color and Attend TF condition separately. The changes in both eccentricity and size are more pronounced when attending changes in color versus TF in the bar. This pattern is most clear in the 'super subject' and 'over subjects' method (albeit with larger variance), and is present in most individual subjects. Error bars reflect 95% CIs across voxels in the 'super subject' and 'per subject' methods, and across subjects in the 'over subjects' method. See Methods section for definition of 'super subject', 'over subjects' and 'per subject' methods.

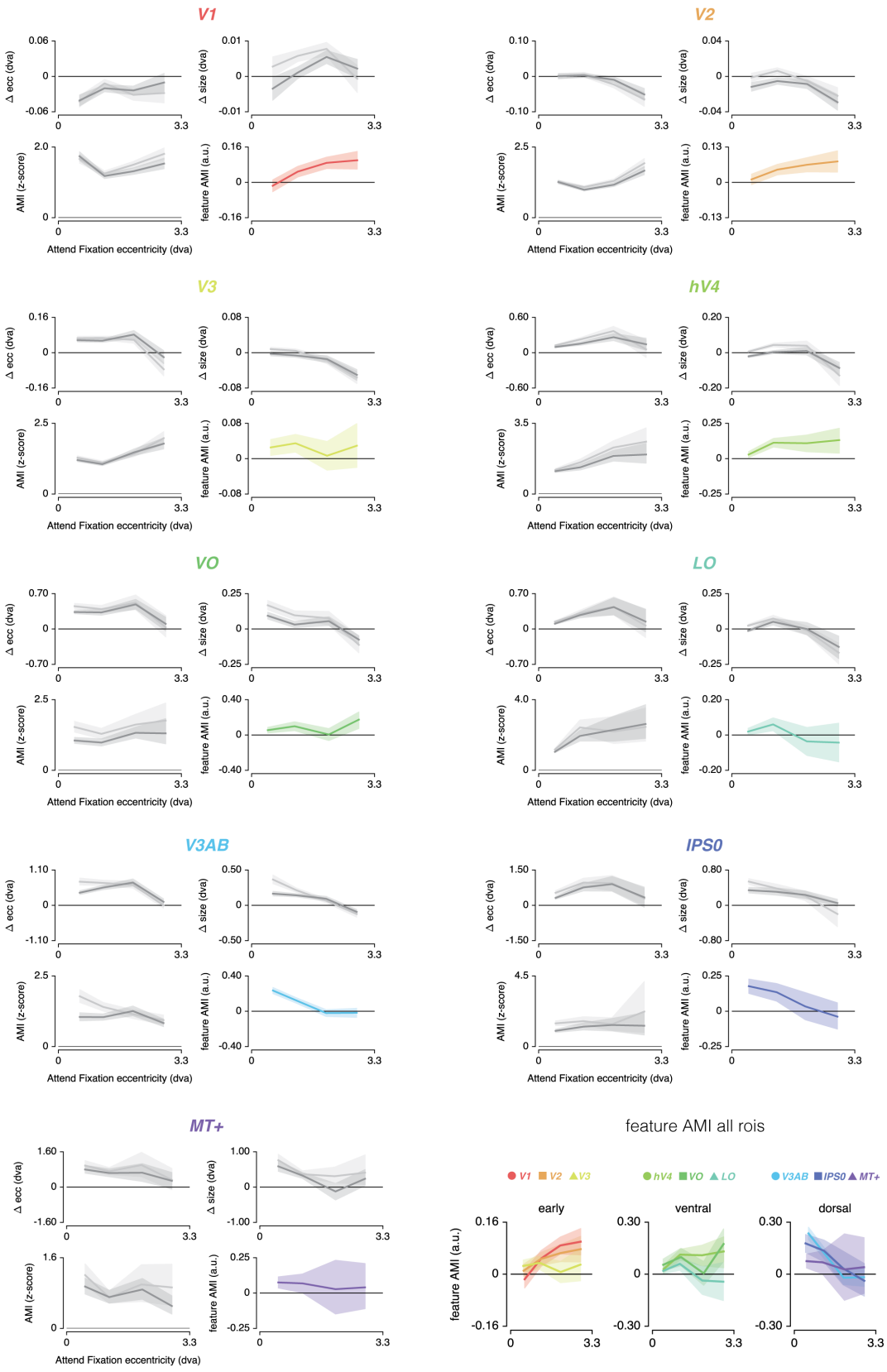

Figure 6 – figure supplement 2. Feature-based attentional modulation of pRF parameters across eccentricity for each individual ROI for the 'super subject'. The

bottom-right panel shows the feature AMI for all ROIs together. This shows that feature-AMI is generally positive along eccentricity across ROIs. In addition, differences in this pattern between ROIs are comparable to differences in the magnitude of pRF changes that resulted from differential spatial attention (Figure 4). Figure 5 showed that these differential patterns along eccentricity are well explained using a similar attentional influence across visual regions. This means that differential feature-AMI patterns along eccentricity are likely the result of differential pRF center and size distributions between ROIs. Inspecting differences in feature-AMI between visual regions should therefore be inspected as an average across the visual field (as presented in Figure 6D and E). Error bars denote 95% CI over voxels.

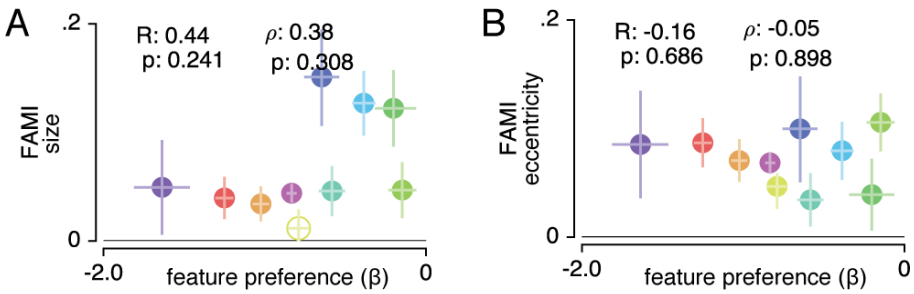

Figure 6 - figure supplement 3. Feature AMI compared to feature preference across ROIs with different ways of computing the FAMI. In A, FAMI only includes the change in pRF size, whereas in B, FAMI only includes the change in pRF eccentricity. This reveals comparable results to when using the combined FAMI pRF size and eccentricity measure. This corroborates that changes in pRF eccentricity and size are closely coupled, warranting the combination of both measures into a single attentional index as presented in the main figure. Error bars denote 95% CI over voxels. Filled markers indicate a significant deviation from 0 with FDR corrected $p < .05$

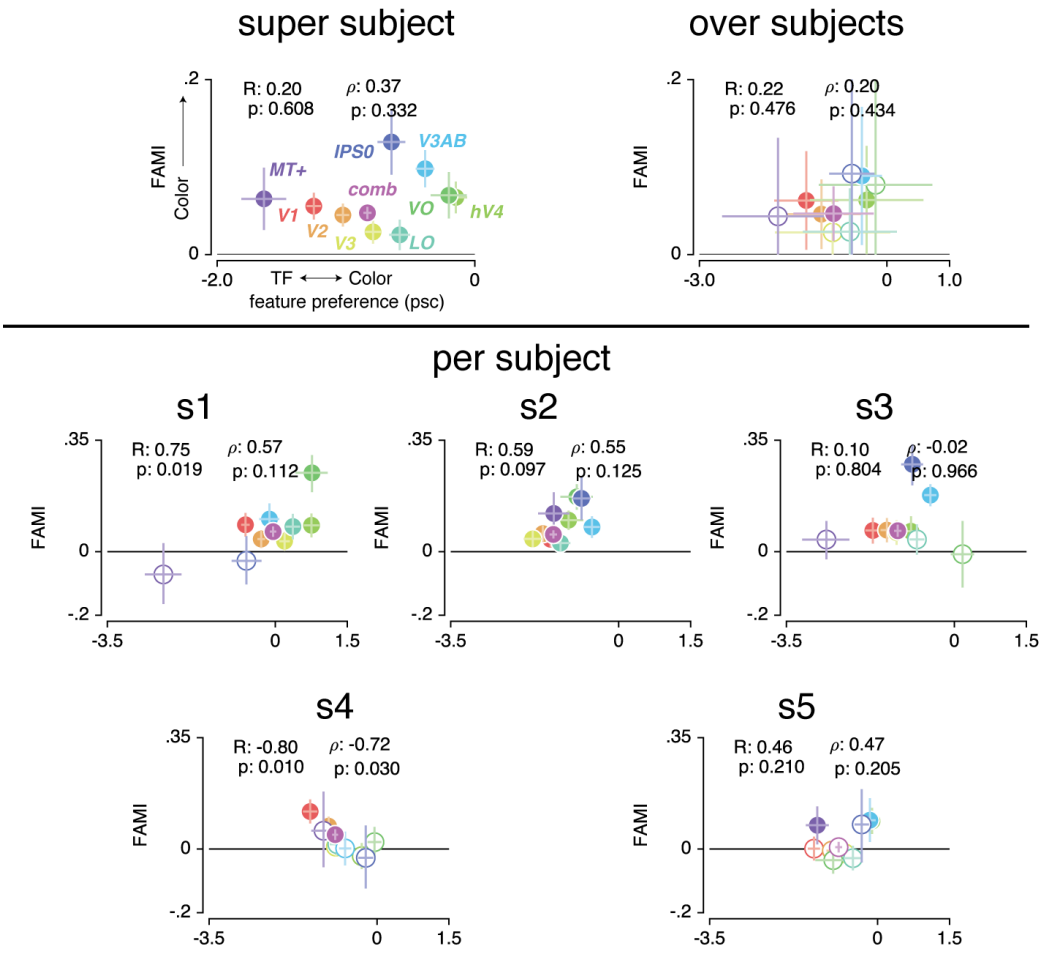

Figure 6 - figure supplement 4. Feature AMI compared to feature preference for each ROI, for each statistical method. The y-axis displays feature AMI, which increases when pRF modulations (size and eccentricity changes combined, see Methods) are greater when attending color compared to TF. The x-axis displays feature preference, which increases with higher color compared to TF preference. pRF modulations were greater when attending color in all ROIs in the 'super subject' method, and was unrelated to feature preference (see Table 9). In the 'over subjects' method, we confirm that feature AMI was not different between ROIs (RM ANOVA, factor of ROI: $F_{(8,32)} = 0.631$, $p = .746$, $\eta^2 p = .066$), and that it was on average 0.059 over ROIs across subjects, $F_{(1,4)} = 18.868$, $p = .012$, $\eta^2 p = .394$). Additionally, we found that for the 'over subjects' method, feature AMI was significantly positive in the combined ROI $t_{(4)} = 4.316$, $p = 0.012$, Cohen's $d = 2.158$ (see Table 25 for all ROIs). Finally, we also found no correlation with feature preference in the 'over subjects' method (mean Spearman correlation = .20, $t_{(4)} = 0.850$, $p = .434$, Cohen's $d = 0.446$; mean Pearson correlation = 0.22, $t_{(4)} = 0.770$, $p = 0.476$, Cohen's $d = 0.429$). Error bars reflect 95% CIs across voxels in the 'super subject' and 'per subject' methods, and across subjects in the 'over

subjects' method. See Methods section for definition of 'super subject', 'over subjects' and 'per subject' methods.

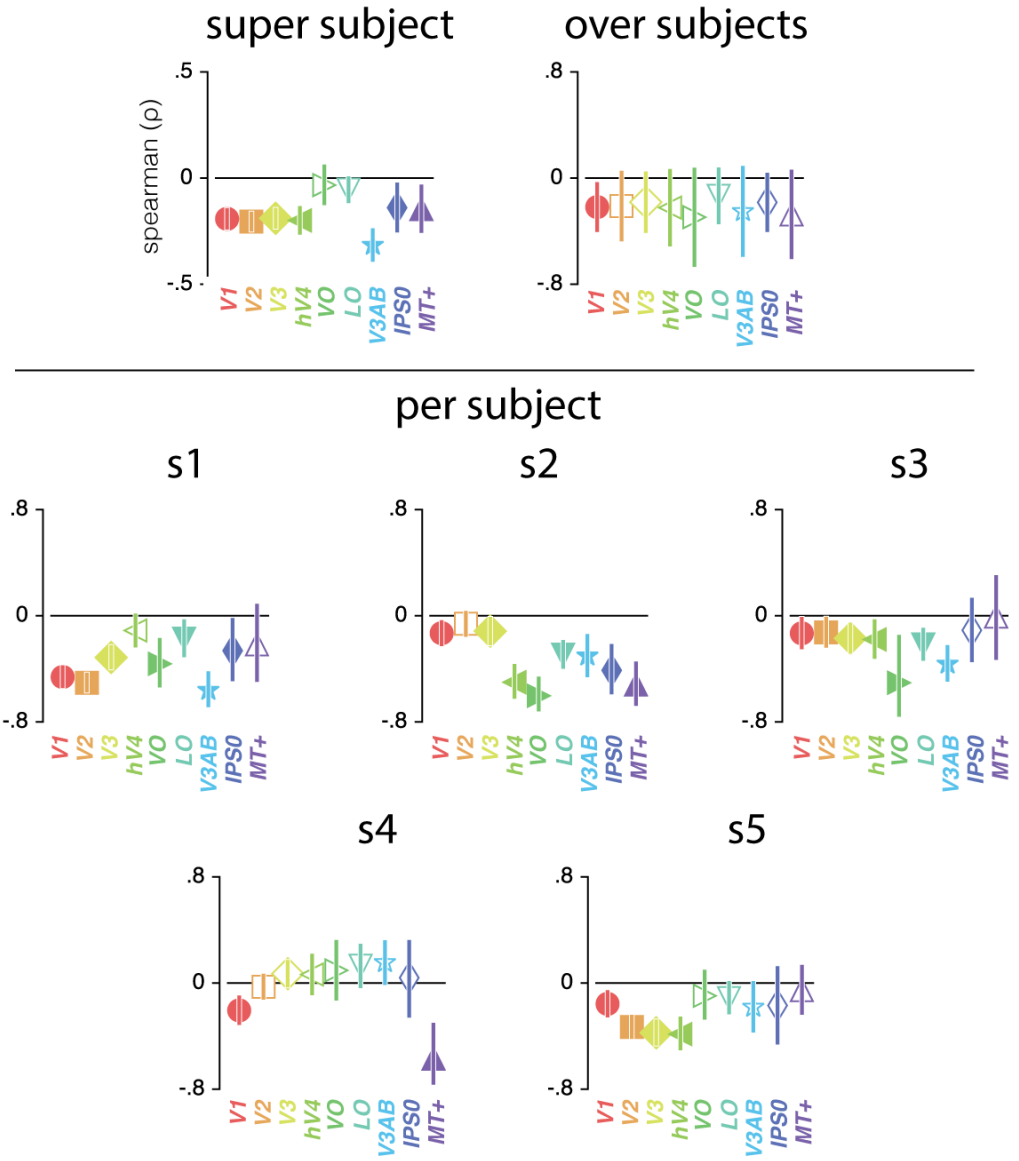

Figure 7 - figure supplement 1. Color compared to TF preference versus eccentricity Spearman correlations. The 'super subject' method shows negative correlations in all ROIs except VO and LO (see Table 10). The 'over subjects' method shows that this correlation is negative on average and does not vary across ROI (RM ANOVA with main factor of ROI $F_{(8,32)} = 0.354$, $p = .937$, $\eta^2 p = .030$, on average -0.22 over ROIs, $F_{(1,4)} = 15.630$, $p = .017$, $\eta^2 p = .641$). When looking at individual subjects, we find that correlations are positive in at least two but often in the majority of subjects across ROIs (see Table 26). Error bars reflect 95% CIs across voxels in the 'super subject' and 'per subject' methods, and across subjects in the 'over subjects' method. See Methods section for definition of 'super subject', 'over subjects' and 'per subject' methods.

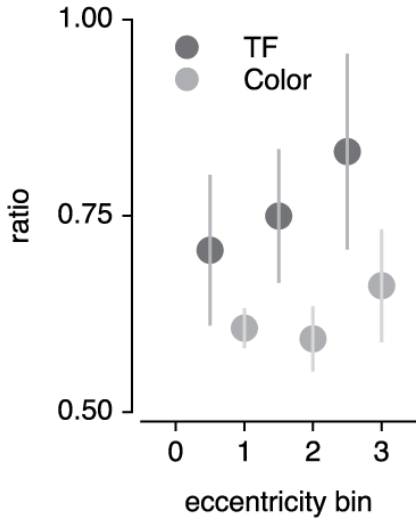

Figure 9 – figure supplement 1. Ratio of Gabor elements of either feature value used by the Quest procedure in order to equate difficulty. In the *Attend Color* condition, this reflected the ratio of elements that were either blue/yellow or green/magenta. In the *Attend TF* condition this reflected the ratio of elements that were either the high or low TF. A RM ANOVA returned a main effect of eccentricity ($F_{(2,8)} = 6.515$, $p = .021$, $\eta^2 p = .620$), a main effect of condition ($F_{(1,4)} = 31.025$, $p = .005$, $\eta^2 p = .886$) and no interaction between eccentricity and condition ($F_{(2,8)} = 1.323$, $p = .319$, $\eta^2 p = .249$). First, this shows (as expected) that in order to equate difficulty, the ratio of elements with the target feature value increased with eccentricity. In addition, it shows that that the number of elements with either high or low temporal frequency was higher than the ratio of elements that was either blue/yellow or green/magenta. This suggests that the two temporal frequencies used in our experiment were perceptually more similar than the two color combinations. Importantly however, the Quest procedure successfully eliminated any effects of this potential difference on task difficulty between conditions (see results on accuracy, Figure 9A). The lack of interaction between attention condition and eccentricity is at apparent odds with the observed decreasing relative preference for color compared to temporal frequency with increasing eccentricity (Figure 7). This could suggest that the greater degree of spatial resampling we observed when attending color discounted the lower relative sensitivity for color in the periphery.